Current Biology 23, 782–787, May 6, 2013 ©2013 Elsevier Ltd All rights reserved http://dx.doi.org/10.1016/j.cub.2013.03.043

Report

Doxorubicin Enhances Nucleosome Turnover around Promoters

Fan Yang,[1] Christopher J. Kemp,[2,*] and Steven Henikoff[1,3,*]
[1]Basic Science Division
[2]Human Biology Division
Fred Hutchinson Cancer Research Center, Seattle, WA 98109, USA
[3]Howard Hughes Medical Institute, Seattle, WA 98109, USA

Summary

Doxorubicin is an anthracycline DNA intercalator that is among the most commonly used anticancer drugs [1]. Doxorubicin causes DNA double-strand breaks in rapidly dividing cells, although whether it also affects general chromatin properties is unknown. Here, we use a metabolic labeling strategy to directly measure nucleosome turnover [2] to examine the effect of doxorubicin on chromatin dynamics in squamous cell carcinoma cell lines derived from genetically defined mice. We find that doxorubicin enhances nucleosome turnover around gene promoters and that turnover correlates with gene expression level. Consistent with a direct action of doxorubicin, enhancement of nucleosome turnover around promoters gradually increases with time of exposure to the drug. Interestingly, enhancement occurs both in wild-type cells and in cells lacking either the *p53* tumor suppressor gene or the master regulator of the DNA damage response, *ATM*, suggesting that doxorubicin action on nucleosome dynamics is independent of the DNA damage checkpoint. In addition, another anthracycline drug, aclarubicin, shows similar effects on enhancing nucleosome turnover around promoters. Our results suggest that anthracycline intercalation promotes nucleosome turnover around promoters by its effect on DNA topology, with possible implications for mechanisms of cell killing during cancer chemotherapy.

Results and Discussion

Nucleosomes Turnover around Gene Promoters

In order to directly measure nucleosome turnover, our lab developed the CATCH-IT (*c*ovalent *a*ttachment to *t*ags to *c*apture *h*istones and *i*dentify *t*urnover) method [2], whereby newly synthesized proteins are labeled with a methionine (Met) analog, azidohomoalanine (Aha), which allows coupling to biotin for affinity capture of purified chromatin. Extraction of DNA from the resulting newly synthesized nucleosomes is followed by genome-wide mapping using tiling microarrays or short-read massively parallel sequencing [3]. We previously applied CATCH-IT to investigate nucleosome changes during the heat-shock response in *Drosophila* cells and discovered that global changes in turnover were associated with transcription without corresponding changes in nucleosome occupancy [4]. The high sensitivity of the CATCH-IT assay to changes in genome-wide chromatin dynamics encouraged us to examine other possible chromatin perturbations using CATCH-IT, such as those that are induced by chemotherapeutic agents. Because doxorubicin (also called adriamycin) is a widely used anticancer drug that interacts directly with DNA, we wondered whether chromatin dynamics are affected by doxorubicin in cancer cells. Accordingly, we applied CATCH-IT to genetically defined mouse squamous cell carcinoma (SCC) cell lines before and after doxorubicin treatment. These cell lines were derived from SCCs induced by the two-step 7,12-dimethylbenz[α]anthracene (DMBA) and 12-O-tetradecanoylphorbol-13-acetate (TPA) carcinogenesis protocol applied to the dorsal skin of mice [5, 6]. Using this protocol, tumors consistently harbor activating mutations in the oncogene *Hras1*.

We first applied CATCH-IT to mouse SCC cells [7]. Sequencing of exons 2–11 of the *p53* gene revealed no mutations, and these cells were designated *p53* wild-type (WT) MSCC-CK1 cells. CATCH-IT and input DNAs were labeled with Cy5 and Cy3, respectively, and were hybridized together to high-density mouse promoter arrays. Gene 5′ or 3′ ends analysis was performed by aligning all annotated mouse genes at transcriptional start sites (TSSs) or transcriptional end sites (TESs) and calculating average nucleosome turnover in 50 bp intervals over a range of 3 kb upstream and 3 kb downstream, using a 200 bp sliding window. As shown in Figure 1A, nucleosome turnover is most rapid around TSSs, decreasing toward gene bodies, consistent with results in *Drosophila* S2 cells [2]. Additionally, strong enrichment was observed upstream of TSSs (Figure 1A). This double-peak pattern is in good agreement with profiles of H3.3, H2A.Z, and many histone modifications associated with active genes in both mouse and human cells [8–11], possibly driven by bidirectional transcription of mammalian promoters. Examples of CATCH-IT profiles are shown for two transcriptionally active genes (*p21* and *Mdm2*), where strong CATCH-IT signals were observed around TSSs in the Aha sample but not in the Met control (Figure 1B).

Nucleosome Turnover Correlates with Transcription

We had previously shown that nucleosome turnover is correlated with gene expression in *Drosophila* cells [2, 4]. To ascertain whether there is a similar relationship between turnover and gene expression in SCC cells, we used microarrays to obtain gene expression profiles. We first compared untreated SCC cells with cells treated with 0.34 μM doxorubicin for 18 hr [12]. Of the total 18,233 genes, only 192 genes were upregulated more than 2-fold with doxorubicin treatment, and 61 genes were downregulated more than 2-fold. Although a minor effect on gene expression was detected upon doxorubicin treatment, Gene Ontology (GO) analysis revealed that genes related to the DNA damage response and cell-cycle arrest were significantly upregulated (see Figure S1 available online).

To examine the relationship between nucleosome turnover and gene expression, we grouped genes into five quintiles according to their expression levels and performed 5′ ends analysis for the genes in each quintile. In addition, we generated a heatmap of nucleosome turnover over the ±3 kb region surrounding the TSSs. We found that nucleosome turnover is correlated with gene expression level before and after doxorubicin treatment, consistent with previous findings in *Drosophila* cells [2, 4] (Figures 2A and 2B). Therefore,

*Correspondence: cjkemp@fhcrc.org (C.J.K.), steveh@fhcrc.org (S.H.)

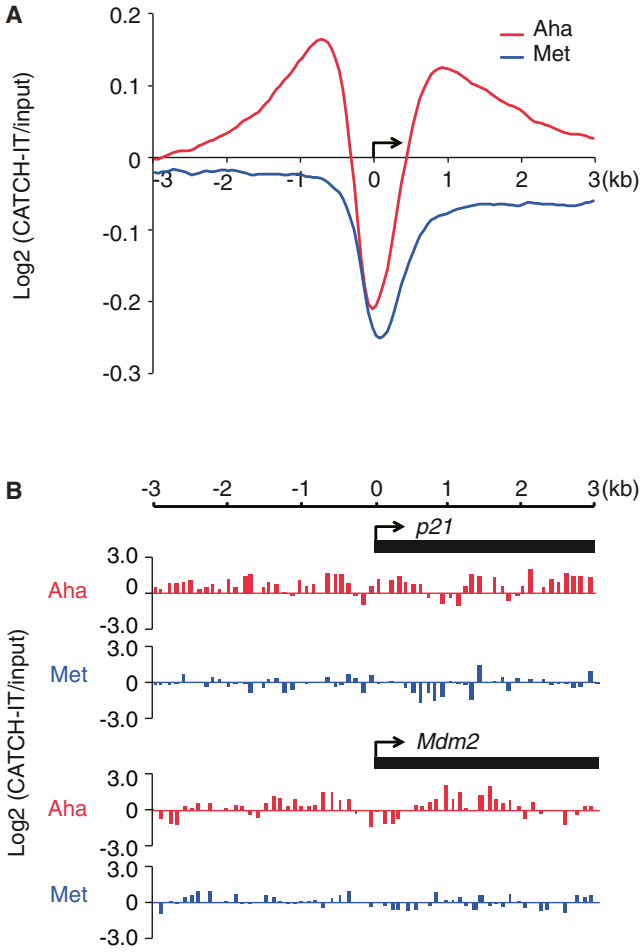

Figure 1. CATCH-IT Analysis of Mouse WT SCC Cells

(A) Average enrichment of CATCH-IT signals at the 5′ ends of 16,797 genes in WT SCC cells (azidohomoalanine [Aha], red curve; methionine [Met], blue curve). Data are shown as $\log_2$ of the average signal ratio between CATCH-IT and input fractions for 3 kb upstream and 3 kb downstream of the transcription start site (TSS; arrow). Data were plotted using a 200 bp sliding window.

(B) CATCH-IT profiles of the promoter regions (±3 kb around the TSS) of two transcriptional active genes (*p21* and *Mdm2*, black boxes) are shown. Data are presented as $\log_2$ ratio between CATCH-IT and input fractions. The TSSs and the transcription direction are marked by arrows. Aha tracks are shown in red; Met tracks are shown in blue.

See also Figure S1.

nucleosome turnover is likely to be coupled to transcription in mammalian cells, as it is in *Drosophila*.

Turnover Increases with Doxorubicin Treatment

To determine whether doxorubicin treatment affects chromatin dynamics, we displayed the difference in nucleosome turnover between treated and untreated cells around 5′ end and 3′ end as a heatmap, ordered by decreasing gene expression. Interestingly, doxorubicin treatment resulted in increased nucleosome turnover almost exclusively at active genes, with the highest levels seen on both sides of the most active gene promoters but not around 3′ ends (Figures 3A and S2A; Table S1). To identify the genes showing enhancement or reduction in turnover in an unbiased manner, we performed unsupervised k-means clustering to separate genes into two groups. About 43% of all mouse annotated genes showed enhancement of nucleosome turnover after doxorubicin treatment (group 1) (Figure 3A). Because only ~1% of all genes showed more than a 2-fold increase in gene expression with doxorubicin treatment, we conclude that this global enhancement in nucleosome turnover around active gene promoters is not a consequence of doxorubicin-induced transcriptional upregulation but is rather a general feature of transcriptional activity in doxorubicin-treated cells.

It is thought that intercalation of doxorubicin into DNA traps topoisomerase II when it is covalently bound to DNA during double-strand cleavage, and that this results in double-strand breaks that must be repaired to avoid chromosome breakage [13]. These breaks induce a strong DNA damage response leading to upregulation of the p53 transcription factor and induction of cell-cycle arrest or apoptosis [12, 14]. Cells lacking p53 are defective in cell-cycle arrest or apoptosis following DNA damage. Because p53 is frequently mutated in human SCC [15, 16] and it is a central player in the cellular response to doxorubicin [17–19], we asked whether doxorubicin-induced increases in nucleosome turnover are dependent on the p53 protein. For this, we developed an SCC cell line derived from a mouse carrying conditional deletion in the *p53* gene [7, 20], designated MSCC-CK4 $Trp53^{-/-}$ (Cre + *Trp53* lox/lox) referred to as $p53^{-/-}$. The cre/lox-mediated deletion of *p53* was confirmed by RT-PCR (Figure S2B). In addition, induction of a well-known p53 transcriptional target, *p21/WAF1* [21], was observed in *p53* WT but not in $p53^{-/-}$ SCC cells after 18 hr of doxorubicin treatment (Figure S2C), further confirming the absence of p53 in $p53^{-/-}$ SCC cells. Furthermore, doxorubicin treatment caused a cell-cycle arrest in the *p53* WT, demonstrating that p53 is active in these cells (Figure S2D). We performed CATCH-IT on $p53^{-/-}$ SCC cells and generated gene expression profiles before and after doxorubicin treatment for 18 hr, as we had done for *p53* WT SCC cells. Similar to the results of expression profiling for *p53* WT cells, only 119 of 18,233 genes were upregulated more than 2-fold, and only 97 genes were downregulated more than 2-fold. As expected for $p53^{-/-}$ cells, GO analysis revealed a lack of DNA-damage response genes among those significantly upregulated (Figure S1). Gene 5′ ends analysis for the genes in each expression quintile and heatmaps ordered by gene expression level were plotted for doxorubicin-treated and untreated $p53^{-/-}$ SCC cells. These plots revealed that in $p53^{-/-}$ SCC cells, nucleosome turnover correlates with gene expression level whether or not the cells were treated with doxorubicin (Figures 2C and 2D).

Similar to what we had observed for *p53* WT SCC cells, nucleosome turnover increased around active gene promoters, but not around 3′ ends, after doxorubicin treatment in about 53% of all mouse annotated genes (group 1) in $p53^{-/-}$ SCC cells (Figure 3B; Table S1). Therefore, p53 is not required for elevation of nucleosome turnover by doxorubicin.

In the above experiments, enhancement of nucleosome turnover was assayed 18 hr after doxorubicin treatment, and it is possible that effects on nucleosome turnover were indirect consequences of intermediate events, such as a global DNA damage response or induction of genes that themselves enhance nucleosome turnover. If, instead, doxorubicin intercalation directly causes nucleosome turnover, then we would expect to see turnover changes gradually increase with time of exposure to the drug. Therefore, we treated WT SCC cells with doxorubicin and performed CATCH-IT on samples at 0, 1, 4, 8, and 24 hr later. As expected for a direct effect of

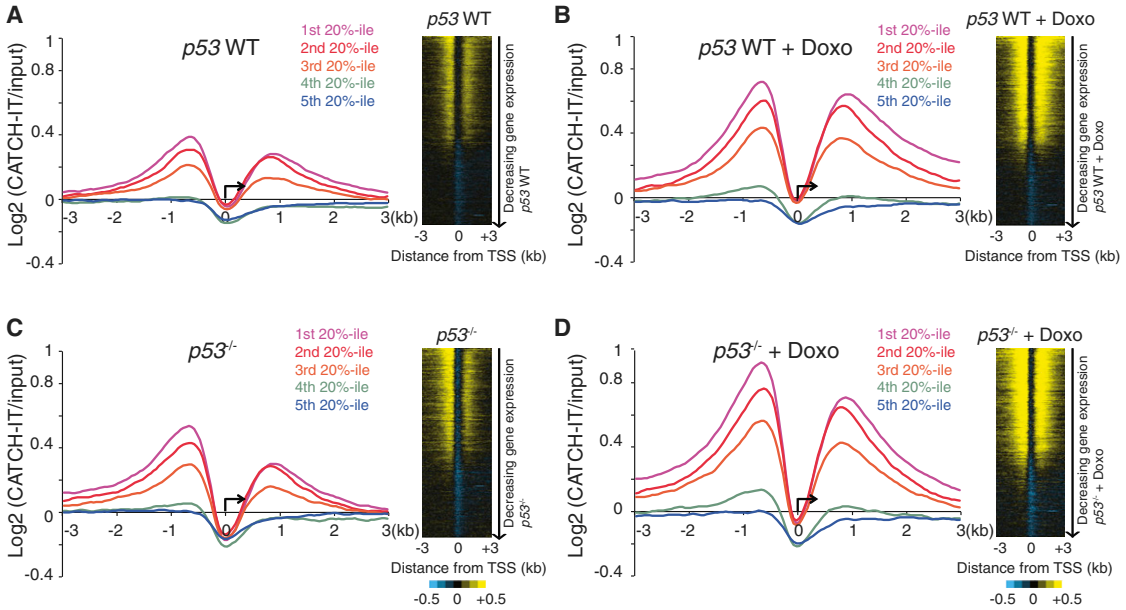

Figure 2. Nucleosome Turnover Correlates with Gene Expression Level in Both *p53* WT and $p53^{-/-}$ SCC Cells before and after Doxorubicin Treatment

Left panels: genes were grouped into five quintiles according to gene expression level (from highest [1st, 20th percentile] to lowest [5th, 20th percentile]) in *p53* WT SCC cells. Ends analysis of average CATCH-IT signals ± 3 kb surrounding the TSS (arrow) was performed for each quintile. Data were plotted using a 200 bp sliding window. Right panels: CATCH-IT data are presented as heatmaps of the ±3 kb surrounding the TSS using Java TreeView. Genes were ordered by decreasing gene expression level in *p53* WT SCC cells (A), doxorubicin (Doxo)-treated *p53* WT SCC cells (B), $p53^{-/-}$ SCC cells (C), and Doxo-treated $p53^{-/-}$ SCC cells (D). The average of two independent experiments is shown in each panel. There is a highly significant excess of genes with an increase in turnover for both WT and $p53^{-/-}$ cells ($p < 10^{-307}$). See also Table S1.

doxorubicin on nucleosome turnover, we found that doxorubicin enhanced nucleosome turnover gradually over the time course (Figures 4A, 4B, and S3; Table S1) .

Enhancement of Turnover Is Independent of the DNA Damage Response

The DNA double-strand breaks induced by doxorubicin treatment activate the ATM kinase that is the master regulator of the DNA damage response [22]. Among other targets, ATM phosphorylates p53 [23] and H2A.X [24] at DNA double-strand breaks and recruits repair proteins to religate the breaks [25–27]. Therefore, we wondered whether ATM is required for the genome-wide enhancement of nucleosome turnover upon doxorubicin treatment. We derived an $ATM^{-/-}$ SCC cell line, MSCC-CK104, from a DMBA/TPA-induced SCC originating in a mouse with a germline mutation in *ATM* [7]. CATCH-IT was performed at 0, 1, 4, 8, and 24 hr after doxorubicin treatment. As shown in Figures 4C and 4D, nucleosome turnover increased gradually upon doxorubicin treatment, indicating that doxorubicin-induced elevation of nucleosome turnover is independent of ATM (Table S1). We conclude that the DNA damage response is not required for the increase in nucleosome turnover induced by doxorubicin.

Aclarubicin Also Enhances Nucleosome Turnover

Doxorubicin is thought to trap covalently bound topoisomerase II at DNA double-strand breakage sites to prevent religation especially when low doses (<1 μM) are used [28]. Breakage by this mechanism is thought to rapidly induce the DNA damage response [19]. To investigate whether topoisomerase II-mediated DNA double-strand breakage is required for the enhancement of nucleosome turnover around promoters, we used another anthracycline drug, aclarubicin (also called aclacinomycin A), which is a DNA intercalator that inhibits topoisomerase activity prior to cleavage, thus not directly resulting in DNA breakage [28]. We first treated WT SCC cells with a series of doses (0.1, 0.2, 0.4, 0.8, 1.6, 3.2, and 6.4 μM) for 24 hr to test for toxicity of aclarubicin. Cell death was observed when treated with 0.8 μM or higher doses (data not shown), consistent with the toxicity seen in human small-cell lung cancer cell lines [29]. CATCH-IT was performed on WT SCC cells after 24 hr aclarubicin treatment at three different doses (0.1, 0.2, and 0.4 μM). Similar to what we had observed for doxorubicin treatment, aclarubicin enhanced nucleosome turnover around promoters of active genes, especially downstream of promoters (Figures 4E and 4F; Table S1). We conclude that direct topoisomerase II-mediated DNA breakage is not required for the observed enhancement of nucleosome turnover.

Conclusions

In summary, we have identified a novel role of widely used chemotherapeutic anthracycline drugs: enhancement of nucleosome turnover around promoters of active genes. This enhancement occurs despite almost undetectable increases in gene expression and is seen in cells that lack both p53 and ATM, which have both been linked to doxorubicin sensitivity [18]. What is the mechanism by which doxorubicin or aclarubicin induces nucleosome turnover around active gene promoters? As DNA intercalators, anthracycline drugs untwist DNA, which in a topologically constrained situation results in positive supercoiling. During transcription initiation, melting of DNA by RNA polymerase would cause the propagation of positive supercoiling on both sides of the promoter, resulting in nucleosome unwrapping [30]. Melting would facilitate intercalation of anthracyclines, thus

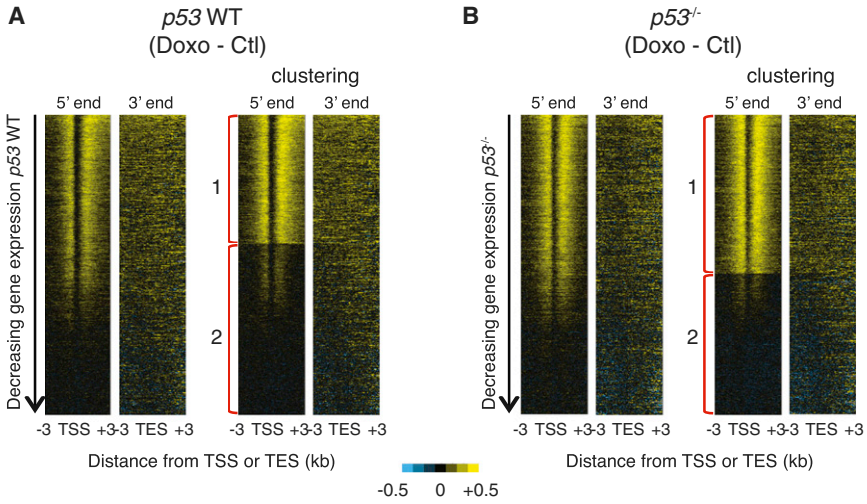

Figure 3. Nucleosome Turnover Is Enhanced around Promoters upon Doxorubicin Treatment in Both *p53* WT and $p53^{-/-}$ SCC Cells

Doxorubicin treatment enhances nucleosome turnover around the transcription start site (TSS), but not around the transcription end site (TES). The difference in nucleosome turnover before and after doxorubicin treatment (Doxo − Ctl) in *p53* WT (A) or $p53^{-/-}$ (B) SCC cells is shown as 5′ and 3′ end heatmaps either by ordering genes according to gene expression level in untreated SCC cells (left) or by unsupervised k-means clustering of TSS ± 3 kb data to separate genes into two groups (right). Ctl, control with no doxorubicin treatment. The average of two independent experiments is shown. See also Figure S2.

enhancing positive supercoil propagation and nucleosome unwrapping. In addition, topoisomerases are able to relax positively supercoiled DNA supercoils; thus, inhibition of topoisomerase II by doxorubicin or aclarubicin may also elevate positive torsional stress generated by RNA polymerase II movement [31, 32]. In either case, enhancement of unwrapping should increase nucleosome eviction and replacement that normally occur during active transcription. In this way, the intercalation of anthracyclines will increase turnover independent of changes in gene expression or the DNA damage response.

Based on our new findings, we speculate that enhancement of nucleosome turnover at promoters by anthracycline drugs can result in increased DNA fragility around promoters. Loss of nucleosomes at human telomeres is thought to be responsible for DNA damage and genome instability associated with alternative lengthening of telomeres (ALT) caused by mutations in the H3.3/DAXX/ATRX nucleosome assembly pathway [33]. Considering that the doses we used in our experiments (0.1–0.4 μM) are much lower than doses used in cancer chemotherapy (~5 μM; [34]), DNA fragility and breakage caused by nucleosome turnover around promoters might contribute to cancer cell killing. Our model might also account for the observation that aclarubicin causes DNA damage in a *Drosophila* in vivo assay [35], despite its inhibition of topoisomerase II activity prior to DNA cleavage. Understanding the molecular effects of anthracycline drug treatment on nucleosome dynamics may provide new insights into the design of anticancer therapies that combine new classes of drugs that target chromatin regulators with traditional chemotherapeutic agents.

Experimental Procedures

Cell Lines

Squamous cell carcinomas were induced by treatment with the carcinogens DMBA and TPA on the dorsal skin of mice carrying germline mutations in *ATM* or *p53*, as well as in WT mice [7]. Tumors arising from this protocol uniformly harbor activating mutations in the oncogene *Hras1*. When tumors underwent malignant papilloma-to-carcinoma conversion, tumors were explanted into culture. Carcinoma cells from the above genotypes were cultured and frozen down at early passage.

Tissue Culture

Mouse SCC cell lines (MSCC-CK1, WT; MSCC-CK4, $p53^{-/-}$; MSCC-CK104, $ATM^{-/-}$) were cultured in Dulbecco's modified Eagle's medium (DMEM) (#11965-092; Invitrogen) supplemented with 10% FBS and 1% penicillin-streptomycin at 37°C.

Cell-Cycle Analysis

WT SCC cells after 18 hr doxorubicin treatment were washed in 1× PBS and fixed in 70% ethanol for about 2 hr. After fixation, cells were washed in 1× PBS, resuspended in 1 ml of propidium iodide (PI) staining solution (1× PBS, 0.1% Triton X-100, 20 μg/ml PI, 100 mg/ml DNase-free RNase A), and incubated at room temperature for 30 min. Flow cytometric analysis was performed utilizing a BD FACS Canto II (Becton Dickinson). Cell-cycle analysis was performed with CellQuest software (Becton Dickinson).

CATCH-IT

CATCH-IT was performed as described previously [2] with some modifications. Briefly, tissue culture medium was replaced with DMEM without methionine (catalog #21013-024; Invitrogen) supplemented with 1× glutamine, 0.2 mM L-cysteine, 10% FBS, and 1% penicillin-streptomycin, and cells were grown at 37°C for starvation for 30 min, followed by 30 min incubation at 37°C with 4 mM azidohomoalanine (catalog #63669; AnaSpec) added to the media. Cells were then harvested, washed with 1× PBS, and resuspended in ice-cold TM2 buffer (10 mM Tris [pH 7.5], 2 mM $MgCl_2$). Cells were lysed using 0.2% of NP-40 and nuclei were isolated, followed by digestion of micrococcal nuclease for 10 min to produce mostly mononucleosomes. Biotin coupling, chromatin extraction, streptavidin pull-down, urea wash, and DNA isolation were then performed as described previously [2].

Microarray Preparation and Data analysis

Input and CATCH-IT DNAs were amplified using a whole-genome amplification kit (catalog #WGA2; Sigma-Aldrich), followed by labeling using Cy3 and Cy5 heptamers according to the Roche Nimblegen labeling protocol. Labeled samples were hybridized together to mouse 2.1-million probe promoter arrays (Roche Nimblegen). For data analysis, arrays were corrected for dye bias [36], and ends analysis, k-mean clustering, and heatmaps were performed as described previously [37].

RNA Isolation, RT-PCR, and Gene Expression Analysis

Total RNA was isolated using the QIAGEN RNeasy kit. For RT-PCR analysis, first-strand cDNA was synthesized using SuperScript II Reverse Transcriptase (Invitrogen), followed by PCR using a set of p53 primers: forward, 5′-GCTTCTCCGAAGACTGGATGACT-3′; reverse, 5′-GATTGTGTCTCAGCC CTGAAGTCA-3′. For expression array analysis, first-strand and second-strand cDNAs were synthesized and double-strand cDNAs were labeled according to the NimbleGen protocol for expression arrays. Labeled samples were hybridized to NimbleGen mouse 385K expression arrays. All samples were normalized together using the robust multichip average (RMA) analysis function provided by DEVA software (NimbleGen). GO analysis was performed by using GeneCodis [38–40].

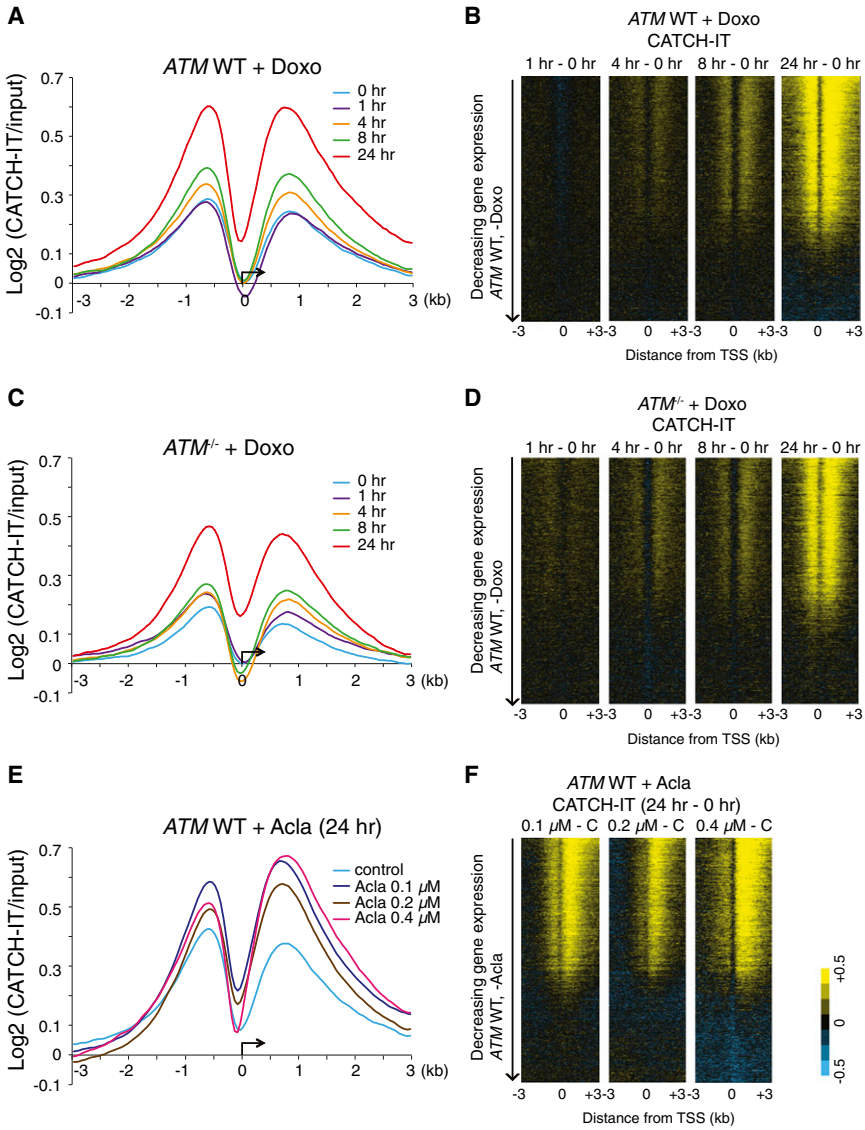

Figure 4. Both Doxorubicin and Aclarubicin Enhance Nucleosome Turnover around Promoters of Active Genes

(A, C, and E) Ends analysis of average enrichment of CATCH-IT signals ± 3 kb surrounding the TSS (arrow) in *ATM* WT (A) and *ATM*$^{-/-}$ (C) SCC cells at 0, 1, 4, 8, and 24 hr after doxorubicin treatment, or in *ATM* WT SCC cells before and after 24 hr aclarubicin treatment at 0.1, 0.2, and 0.4 μM (E). Data were plotted using a 200 bp sliding window. (B, D, and F) Differences in nucleosome turnover between doxorubicin-treated *ATM* WT (B) or *ATM*$^{-/-}$ (D) SCC cells (treated for 1, 4, 8, or 24 hr) and untreated *ATM* WT or *ATM*$^{-/-}$ SCC cells (0 hr) or between aclarubicin-treated *ATM* WT (treated at 0.1, 0.2, and 0.4 μM) and untreated *ATM* WT (control) SCC cells (F) are shown as heatmaps. Genes were ordered by decreasing gene expression in *ATM* WT SCC cells without doxorubicin or aclarubicin treatment. Except for the 1 hr time points, there is a highly significant excess of genes with an increase in turnover (Table S1).

See also Figure S3.

Accession Numbers

The microarray data from this study have been submitted to the NCBI Gene Expression Omnibus under the accession number GSE43753.

Supplemental Information

Supplemental Information includes three figures and one table and can be found with this article online at http://dx.doi.org/10.1016/j.cub.2013.03.043.

Acknowledgments

We thank Kay E. Gurley for isolating mouse SCC cells, Russell Moser for help with cell culture and cell-cycle analysis, Neil G. Shafer and Andy Marty for processing arrays, and Jorja Henikoff for bioinformatics. This work was supported by NIH grant R01 ES020116 (S.H. and C.J.K.), the Howard Hughes Medical Institute (S.H.), and NIH grant U54 CA143862 (S.H.).

Received: December 20, 2012
Revised: March 3, 2013
Accepted: March 18, 2013
Published: April 18, 2013

References

1. Denny, W.A. (1989). DNA-intercalating ligands as anti-cancer drugs: prospects for future design. Anticancer Drug Des. *4*, 241–263.
2. Deal, R.B., Henikoff, J.G., and Henikoff, S. (2010). Genome-wide kinetics of nucleosome turnover determined by metabolic labeling of histones. Science *328*, 1161–1164.
3. Teves, S.S., Deal, R.B., and Henikoff, S. (2012). Measuring genome-wide nucleosome turnover using CATCH-IT. Methods Enzymol. *513*, 169–184.
4. Teves, S.S., and Henikoff, S. (2011). Heat shock reduces stalled RNA polymerase II and nucleosome turnover genome-wide. Genes Dev. *25*, 2387–2397.
5. Kemp, C.J. (2005). Multistep skin cancer in mice as a model to study the evolution of cancer cells. Semin. Cancer Biol. *15*, 460–473.
6. Abel, E.L., Angel, J.M., Kiguchi, K., and DiGiovanni, J. (2009). Multi-stage chemical carcinogenesis in mouse skin: fundamentals and applications. Nat. Protoc. *4*, 1350–1362.
7. Bailey, S.L., Gurley, K.E., Hoon-Kim, K., Kelly-Spratt, K.S., and Kemp, C.J. (2008). Tumor suppression by p53 in the absence of Atm. Mol. Cancer Res. *6*, 1185–1192.
8. Barski, A., Cuddapah, S., Cui, K., Roh, T.Y., Schones, D.E., Wang, Z., Wei, G., Chepelev, I., and Zhao, K. (2007). High-resolution profiling of histone methylations in the human genome. Cell *129*, 823–837.

9. Barski, A., Chepelev, I., Liko, D., Cuddapah, S., Fleming, A.B., Birch, J., Cui, K., White, R.J., and Zhao, K. (2010). Pol II and its associated epigenetic marks are present at Pol III-transcribed noncoding RNA genes. Nat. Struct. Mol. Biol. *17*, 629–634.
10. Ku, M., Jaffe, J.D., Koche, R.P., Rheinbay, E., Endoh, M., Koseki, H., Carr, S.A., and Bernstein, B.E. (2012). H2A.Z landscapes and dual modifications in pluripotent and multipotent stem cells underlie complex genome regulatory functions. Genome Biol. *13*, R85.
11. Goldberg, A.D., Banaszynski, L.A., Noh, K.M., Lewis, P.W., Elsaesser, S.J., Stadler, S., Dewell, S., Law, M., Guo, X., Li, X., et al. (2010). Distinct factors control histone variant H3.3 localization at specific genomic regions. Cell *140*, 678–691.
12. Attardi, L.D., de Vries, A., and Jacks, T. (2004). Activation of the p53-dependent G1 checkpoint response in mouse embryo fibroblasts depends on the specific DNA damage inducer. Oncogene *23*, 973–980.
13. Vos, S.M., Tretter, E.M., Schmidt, B.H., and Berger, J.M. (2011). All tangled up: how cells direct, manage and exploit topoisomerase function. Nat. Rev. Mol. Cell Biol. *12*, 827–841.
14. Vousden, K.H., and Lu, X. (2002). Live or let die: the cell's response to p53. Nat. Rev. Cancer *2*, 594–604.
15. Poeta, M.L., Manola, J., Goldwasser, M.A., Forastiere, A., Benoit, N., Califano, J.A., Ridge, J.A., Goodwin, J., Kenady, D., Saunders, J., et al. (2007). TP53 mutations and survival in squamous-cell carcinoma of the head and neck. N. Engl. J. Med. *357*, 2552–2561.
16. Agrawal, N., Frederick, M.J., Pickering, C.R., Bettegowda, C., Chang, K., Li, R.J., Fakhry, C., Xie, T.X., Zhang, J., Wang, J., et al. (2011). Exome sequencing of head and neck squamous cell carcinoma reveals inactivating mutations in NOTCH1. Science *333*, 1154–1157.
17. Jackson, J.G., Pant, V., Li, Q., Chang, L.L., Quintás-Cardama, A., Garza, D., Tavana, O., Yang, P., Manshouri, T., Li, Y., et al. (2012). p53-mediated senescence impairs the apoptotic response to chemotherapy and clinical outcome in breast cancer. Cancer Cell *21*, 793–806.
18. Jiang, H., Reinhardt, H.C., Bartkova, J., Tommiska, J., Blomqvist, C., Nevanlinna, H., Bartek, J., Yaffe, M.B., and Hemann, M.T. (2009). The combined status of ATM and p53 link tumor development with therapeutic response. Genes Dev. *23*, 1895–1909.
19. Kurz, E.U., Douglas, P., and Lees-Miller, S.P. (2004). Doxorubicin activates ATM-dependent phosphorylation of multiple downstream targets in part through the generation of reactive oxygen species. J. Biol. Chem. *279*, 53272–53281.
20. Bornachea, O., Santos, M., Martínez-Cruz, A.B., García-Escudero, R., Dueñas, M., Costa, C., Segrelles, C., Lorz, C., Buitrago, A., Saiz-Ladera, C., et al. (2012). EMT and induction of miR-21 mediate metastasis development in Trp53-deficient tumours. Sci. Rep. *2*, 434.
21. Laptenko, O., Beckerman, R., Freulich, E., and Prives, C. (2011). p53 binding to nucleosomes within the p21 promoter in vivo leads to nucleosome loss and transcriptional activation. Proc. Natl. Acad. Sci. USA *108*, 10385–10390.
22. Shiloh, Y. (2006). The ATM-mediated DNA-damage response: taking shape. Trends Biochem. Sci. *31*, 402–410.
23. Canman, C.E., Lim, D.S., Cimprich, K.A., Taya, Y., Tamai, K., Sakaguchi, K., Appella, E., Kastan, M.B., and Siliciano, J.D. (1998). Activation of the ATM kinase by ionizing radiation and phosphorylation of p53. Science *281*, 1677–1679.
24. Burma, S., Chen, B.P., Murphy, M., Kurimasa, A., and Chen, D.J. (2001). ATM phosphorylates histone H2AX in response to DNA double-strand breaks. J. Biol. Chem. *276*, 42462–42467.
25. Bonner, W.M., Redon, C.E., Dickey, J.S., Nakamura, A.J., Sedelnikova, O.A., Solier, S., and Pommier, Y. (2008). GammaH2AX and cancer. Nat. Rev. Cancer *8*, 957–967.
26. Svetlova, M., Solovjeva, L., Nishi, K., Nazarov, I., Siino, J., and Tomilin, N. (2007). Elimination of radiation-induced gamma-H2AX foci in mammalian nucleus can occur by histone exchange. Biochem. Biophys. Res. Commun. *358*, 650–654.
27. Siino, J.S., Nazarov, I.B., Svetlova, M.P., Solovjeva, L.V., Adamson, R.H., Zalenskaya, I.A., Yau, P.M., Bradbury, E.M., and Tomilin, N.V. (2002). Photobleaching of GFP-labeled H2AX in chromatin: H2AX has low diffusional mobility in the nucleus. Biochem. Biophys. Res. Commun. *297*, 1318–1323.
28. Pommier, Y., Leo, E., Zhang, H., and Marchand, C. (2010). DNA topoisomerases and their poisoning by anticancer and antibacterial drugs. Chem. Biol. *17*, 421–433.
29. Jensen, P.B., Sørensen, B.S., Demant, E.J., Sehested, M., Jensen, P.S., Vindeløv, L., and Hansen, H.H. (1990). Antagonistic effect of aclarubicin on the cytotoxicity of etoposide and 4′-(9-acridinylamino)methanesulfon-m-anisidide in human small cell lung cancer cell lines and on topoisomerase II-mediated DNA cleavage. Cancer Res. *50*, 3311–3316.
30. Zlatanova, J., and Victor, J.M. (2009). How are nucleosomes disrupted during transcription elongation? HFSP J. *3*, 373–378.
31. Liu, L.F., and Wang, J.C. (1987). Supercoiling of the DNA template during transcription. Proc. Natl. Acad. Sci. USA *84*, 7024–7027.
32. Wu, H.Y., Shyy, S.H., Wang, J.C., and Liu, L.F. (1988). Transcription generates positively and negatively supercoiled domains in the template. Cell *53*, 433–440.
33. Lovejoy, C.A., Li, W., Reisenweber, S., Thongthip, S., Bruno, J., de Lange, T., De, S., Petrini, J.H., Sung, P.A., Jasin, M., et al.; ALT Starr Cancer Consortium. (2012). Loss of ATRX, genome instability, and an altered DNA damage response are hallmarks of the alternative lengthening of telomeres pathway. PLoS Genet. *8*, e1002772.
34. Namur, J., Citron, S.J., Sellers, M.T., Dupuis, M.H., Wassef, M., Manfait, M., and Laurent, A. (2011). Embolization of hepatocellular carcinoma with drug-eluting beads: doxorubicin tissue concentration and distribution in patient liver explants. J. Hepatol. *55*, 1332–1338.
35. Lehmann, M., Vilar, Kde.S., Franco, A., Reguly, M.L., and Rodrigues de Andrade, H.H. (2004). Activity of topoisomerase inhibitors daunorubicin, idarubicin, and aclarubicin in the *Drosophila* Somatic Mutation and Recombination Test. Environ. Mol. Mutagen. *43*, 250–257.
36. Peng, S., Alekseyenko, A.A., Larschan, E., Kuroda, M.I., and Park, P.J. (2007). Normalization and experimental design for ChIP-chip data. BMC Bioinformatics *8*, 219.
37. Conerly, M.L., Teves, S.S., Diolaiti, D., Ulrich, M., Eisenman, R.N., and Henikoff, S. (2010). Changes in H2A.Z occupancy and DNA methylation during B-cell lymphomagenesis. Genome Res. *20*, 1383–1390.
38. Tabas-Madrid, D., Nogales-Cadenas, R., and Pascual-Montano, A. (2012). GeneCodis3: a non-redundant and modular enrichment analysis tool for functional genomics. Nucleic Acids Res. *40*(Web Server issue), W478–W483.
39. Carmona-Saez, P., Chagoyen, M., Tirado, F., Carazo, J.M., and Pascual-Montano, A. (2007). GENECODIS: a web-based tool for finding significant concurrent annotations in gene lists. Genome Biol. *8*, R3.
40. Nogales-Cadenas, R., Carmona-Saez, P., Vazquez, M., Vicente, C., Yang, X., Tirado, F., Carazo, J.M., and Pascual-Montano, A. (2009). GeneCodis: interpreting gene lists through enrichment analysis and integration of diverse biological information. Nucleic Acids Res. *37*(Web Server issue), W317–W322.